ISSN 1816-6075 (Print), 1818-0523 (Online)
Journal of System and Management Sciences
Vol. 13 (2023) No. 1, pp. 63-84
DOI:10.33168/JSMS.2023.0104

Identify Faults in Road Structure Zones with Deep Learning

Yohan Roy Alarcón Cajas, Yenmy Zúñiga Guisado, Afredo Daza Vergaray

Universidad César Vallejo, Carretera Panamericana Norte Km 695, Los Olivos, Lima, Peru

E-mail: yalarconca@ucvvirtual.edu.pe; yzunigag@ucvvirtual.edu.pe; adazave@ucvvirtual.edu.pe

Abstract. One of the most important causes that cause traffic accidents is the deterioration or failures in road structures, which occurs due to the low quality of its components, climate changes, and seismic zones, heavy cargo transport traffic, among others; therefore, the purpose of this research is the detection of faults in the pavement. The set of images used was classified into cracks and gaps, making a total of 420 images. The research was carried out taking into account the following stages: data collection, through a smartphone the images were captured; data preprocessing, which allowed the best images to be selected and redimensioned; model of the network architecture, allowed the selection and improvement of the algorithm; training and verification of the algorithm, to create an optimal model in the detection of cracks and gaps, as a last stage, the deployment, where the system for the test of the model was developed; for which a Convolutional Neural Network (CNN) was used as the YOLOv5 algorithm, using the Adam and 120 optimization algorithm, reaching an accuracy of 58%, validating it then with 30 images, having the averages of 85% accuracy, 91.5 sensitivity and 81.5% F1-Score. Concluding that the algorithm with convolutional neural networks helps to properly identify pavement failures, being important for authorities to do proper maintenance.

Keywords: Deep Learning, Pavement, Cracks and Gaps

1. Introduction

When talking about road structures, they must be in good condition, this because through their main roads they transit trade, the intercommunication of their inhabitants and exchange of different cultures; all this is important for the development and economic growth of a country (Shatnawi, 2018). It is there that the need arises to mitigate the defects that may be generated over time as a result of the weather or heavy cargo transport; therefore, the importance of constant monitoring that maintains the useful life cycle of road structures in good condition, using concrete pavements continuously, in order to mitigate the risks of accidents that may be caused (Shim et al., 2020).

In fact, road defects are caused by different reasons, where car accidents stand out, weakening their components and causing dangerous areas for road traffic (Chun & Ryu, 2019), also known as road structure disease (Zhang et al., 2020); in the same way, aging is another factor that weakens its structural components, therefore its state must be evaluated periodically to identify these failures (cracks or gaps) and thus implement an adequate rehabilitation with quality components (Slami & Yun, 2021), being important that the State or competent authorities intervene in the analysis and corresponding evaluations for the adequate transit of society.

In sum, in many underdeveloped countries, road infrastructure maintenance activities have declined due to the complexity of access to them, bureaucracy or other factors (Silva et al., 2020).

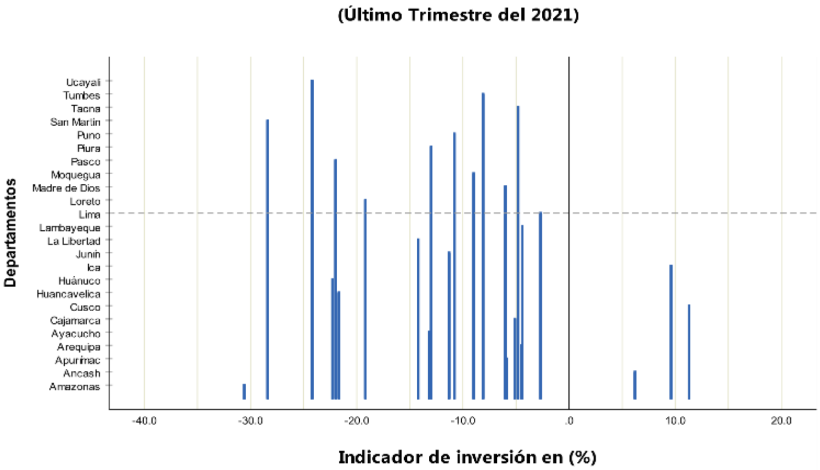

Fig. 1: Registration of the Investment Index Applied in the Construction Sector according to its Geographical Area of Peru (INEI, 2022)

Figure 1 shows the investment in the construction sector according to its geographical area. So much so that, in the last quarter of 2021, investment in structures in Peru was -5.8%, with the indices being the following: In Amazonas it highlighted indicators of -30.6%, unlike Ancash where it registered positive percentages of 6.2%, also Apurimac was below -5.9% and Arequipa at -4.5%, while in Ayacucho it showed indicators of -13.2% of investment, similarly Cajamarca with -5.1%, however Cusco acquired high percentages such as 11.3% in execution of road investments, on the other hand the department of Huancavelica registered -21.7% unlike Huánuco which was -22.3%, compared to Ica where only 9.6% appeared, while in Junín with 11.3%, La Libertad with -14.2%, Lambayeque -4.4%, while, Lima only executed the investment in construction of -2.7% which is a very low indicator in this sector, while Loreto showed an execution of -19.2%, Madre de Dios with -6.0%, as well as in Moquegua it was observed that it was -9.0%, Pasco with -22%, Piura with a record of -13%, Puno -10.8%, followed by San Martin with -28.4%, Tacna -4.8%, Tumbes with -8.1% and finally, Ucayali with -24.2% (National Institute of Statistics and Informatics [INEI], 2022).

As for the budget in the construction sector, it is composed of investments in road structures and their rehabilitation, so it is essential to intervene in technological tools that allow standardizing the identification and analysis of the failures generated in these structures. Therefore, the benefits of technology in this area, specifically artificial intelligence, have been involved in the personal, work and economic activities of man (Backman & Chung, 2021; Opara et al., 2021); highlighting image recognition through deep learning, achieving important developments for society, such as the detection of objects with a high degree of accuracy (Qiao et al., 2021); where neural networks, algorithm architectures, techniques and effective tools that have the ability to learn and recognize patterns to make decisions are used (Sarmiento, 2020; Coluccia, 2021; Morales & Kayacan, 2020).

It is worth mentioning that tests have been carried out with pavement images, achieving positive results in the accuracy for the detection of failures in road structures (He & Liu, 2020; Enzo, 2021), using algorithms such as Depth separable convolution, Atrocious Convolution, Xception-65, Atrous Spatial Pyramid Polling (Sun et al., 2021), algorithm proposed with SegNet (Ramalingamm et al., 2021), ResNet (Fan et al., 2022), proposed algorithm (Maeda et al., 2018), where to date the present study has been carried out, no investigations were found using the Yolo algorithm.

This article is aimed at detecting damage to road structures such as holes and cracks, caused by various reasons, such as the intervention of the human factor, climate changes, seismic zones, transit of heavy cargo transport, which leads to an imminent danger to the population in transport. Likewise, to identify and analyze these failures it was necessary to perform a series of activities such as capturing images through a smartphone that allows us autonomy in data collection, choosing algorithms, training the intelligent model and measuring the results (Morales & Kayacan, 2020; Janani et al., 2022). In this context, the research work is related to identifying failures in road structures in which image processing techniques are applied through convolutional neural networks (CNN) (Kumar et al., 2021; Zhang, 2021). For this, it is required to perform a series of structured steps where algorithms are incorporated that provide data for classification and take this information from the fault or defect.

The document is organized into six sections. Section 2, the review of the works related to the research is carried out. Section 3 contains the methodology. Section 4 shows the results obtained. Section 5 describes the discussion. Finally, section 6 contains the findings of the investigation.

2. Literature Review

The works developed to identify cracks, as well as gaps through Deep Learning consist of authors who obtained highly qualified results with CNN, applied in different studies in order to automatically identify failures of road pavements based on intelligent architectures through image segmentation; this must include a series of algorithms that served as gears to obtain good accuracy (Fan et al. 2022).

However, it should be noted that, in the real field, the inspection of the roads is carried out with topographic equipment, which must be clear for their adequate treatment by specialized agencies, but for image recognition investigations there is no standardization of data that are available, some studies took the method of image collection through smartphones as mentioned (Maeda et al. 2018), while in other research the collection of information was supported by a drone (Kumar et al., 2021).

The various ways of grouping information for image segmentation are essential in the application of CNNs through architectures such as YOLO-v3, among the most widely used (Park et al., 2018). This algorithm was used for crack detection in pavements in three phases that included image processing, machine learning and deep learning. More detail on the algorithms and methods used is provided below.

3. Materials and methods

For the development of this study, it was carried out in four phases: In the first phase, data collection is carried out; The second phase describes the pre-processing of information; as in the third phase, the operation of the YOLO v5 algorithm is explained; continuing with phase four, where the training and verification of the algorithm for the pavement is carried out; and, finally, phase 5 shows the implementation of the system for the validation of the algorithm.

3.1. Data Collection

For the collection of images was carried out following the sequence detailed below:

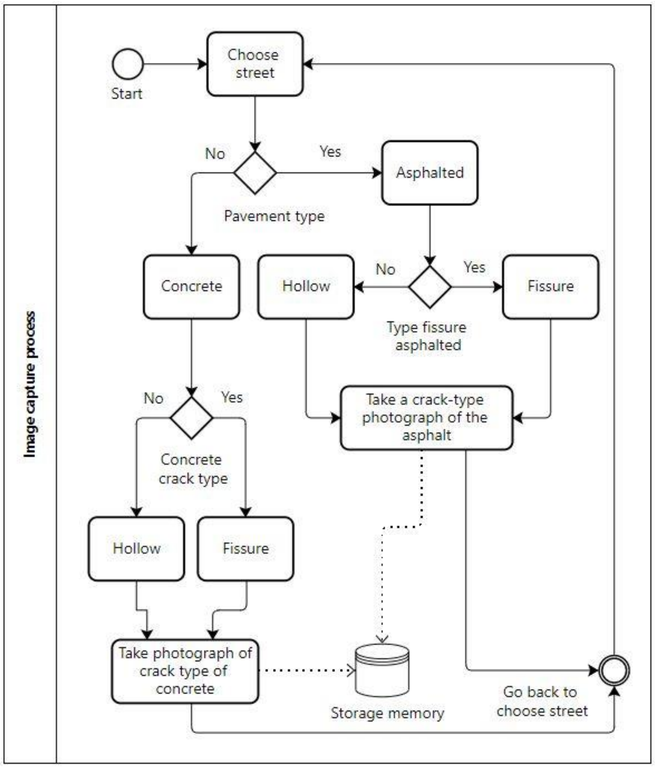

Fig. 2: Image Collection

Figure 2 shows the process of capturing the images, which begins with the selection of the avenue, then the type of pavement (concrete or asphalt) is verified, according to the first two characteristics we proceed with the image capture, where the type of class (crack or hole) is displayed, Finally, the information is stored in the smartphone's memory and the process is restarted in order to capture another image successively in the process.

For the study, 420 images were collected in RGB format through a smartphone, on the pavement of the district of Villa María del Triunfo, for which the camera was positioned at an angle of 15 ° to 45 ° due to the unevenness of the pavements, to capture images of cracks and holes with different characteristics, the same ones that were stored in a memory of 32Gb with the original size of 2160 x 3120 pixels.

Table 1: Collection and recording of image capture features

Class	Fault	Pavement type	Number of images	Total per class
Crack	Transverse carck	Cement	121	292
		Asphalted	12	
	Longitudinal crack	Cement	84	
		Asphalted	8	
	Cocodrile crack	Cement	33	
		Asphalted	34	
Hollow	Manhole cover	Cement	50	128
		Asphalted	78	

Table 1 shows the number of images per class (crack and gap), according to their type of defect and pavement (cement or asphalt), deducing that the largest number of images correspond to the class, with transverse defect and type of cement pavement. Likewise, the least amount of images corresponds to the crack class, with longitudinal defect type of asphalted pavement.

3.2. Data Pre-processing

In the image pre-processing was performed following the sequence as shown below:

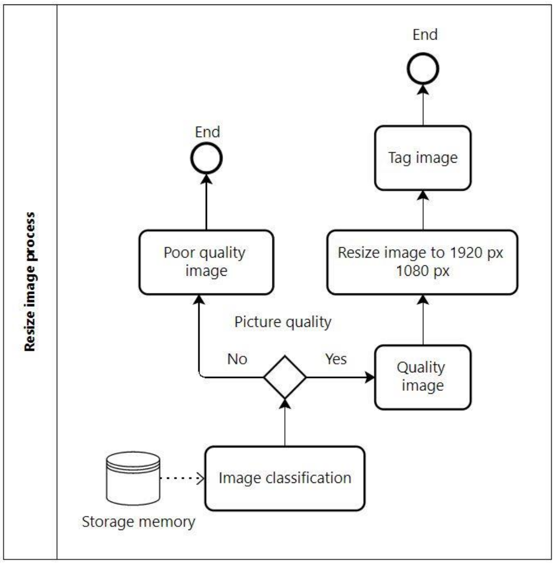

Fig. 3: Image Preprocessing Diagram

In figure 3, the pre-processing began with the classification of the captured images (gap and crack), selecting those with good pixel resolution, then proceeded with the resizing of 1920 pixels by 1080 pixels to maintain the quality of sharpness, using Adobe Inc. software, which improved the mathematical calculations of the

Adam algorithm, as well as max pooling, managing to group the parameters of height, width, type and length of the RGB format, this event being important to improve the performance of each era of the algorithm.

Table 2: Collection of images in different states of cracks and gaps

	Original (4160x3120 px)	Resized image (1920x1080 px)
Crack, on concrete with paint		
Crack on concrete		
Crack on asphalt with shade		
Crack on asphalt including moisture		
Hollow on asphalt, including moisture		
Hole on asphalt		

Table 2 shows some characteristics of the cracks and gaps at the time of data collection; The most outstanding characteristics are the type of material (concrete or asphalt) and conditions (paint, shade or moisture). Likewise, the dimension of the images collected with the smartphone was 4160x3120 pixels, but then it was resized to 1920x1080 pixels.

Then the labeling was carried out as shown in figure 4, where you can see the location of the hole and crack within the image, using the Adobe Cloud tool – MakeAlphaSense.

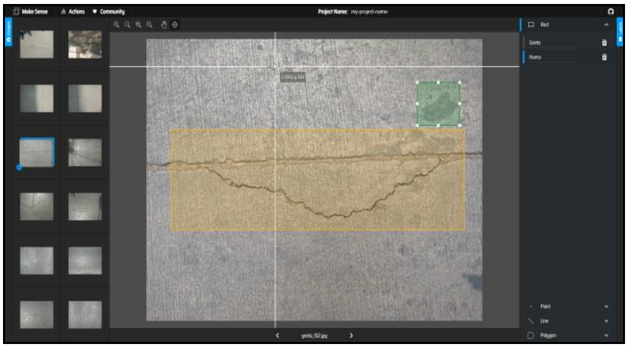

Fig. 4: Image Labeling

In figure 4, the process of labeling the cracks and gaps in the images is observed using the MakeAlphaSense tool, in order to obtain the coordinate of the cracks and gaps in the images as shown in figure 5, which were converted into a matrix to use as input data in the proposed algorithm.

Conversion de imagen a matriz

Clase	Matriz				Nombre de imagen y tipo de extension	Ancho	Altura
Hueco	81	284	1766	330	grieta_1.jpg	1920	1080
Hueco	58	172	1198	447	grieta_10.jpg	1920	1080
Grieta	45	314	1008	223	grieta_100.jpg	1920	1080
Grieta	45	306	1861	301	grieta_101.jpg	1920	1080
Grieta	391	489	1290	302	grieta_102.jpg	1920	1080
Grieta	472	473	468	159	grieta_103.jpg	1920	1080
Hueco	313	418	122	103	grieta_103.jpg	1920	1080
Grieta	742	390	454	193	grieta_104.jpg	1920	1080
Grieta	475	521	232	221	grieta_104.jpg	1920	1080
Grieta	204	291	1663	413	grieta_105.jpg	1920	1080
Grieta	117	750	430	313	grieta_105.jpg	1920	1080
Grieta	405	10	1103	746	grieta_106.jpg	1920	1080
Grieta	19	613	351	176	grieta_106.jpg	1920	1080
Grieta	531	495	175	486	grieta_107.jpg	1920	1080
Grieta	1276	15	276	425	grieta_107.jpg	1920	1080
Grieta	1074	481	209	574	grieta_107.jpg	1920	1080
Grieta	44	221	1800	447	grieta_108.jpg	1920	1080
Grieta	390	423	285	114	grieta_109.jpg	1920	1080
Hueco	355	289	1058	661	grieta_11.jpg	1920	1080
Hueco	1361	69	549	597	grieta_11.jpg	1920	1080
Hueco	47	111	516	257	grieta_11.jpg	1920	1080
Grieta	265	439	957	237	grieta_110.jpg	1920	1080
Grieta	69	323	1727	321	grieta_111.jpg	1920	1080
Hueco	714	448	488	170	grieta_112.jpg	1920	1080
Grieta	614	330	1216	245	grieta_113.jpg	1920	1080
Grieta	59	451	415	207	grieta_113.jpg	1920	1080
Grieta	377	707	142	357	grieta_113.jpg	1920	1080
Grieta	332	389	592	259	grieta_114.jpg	1920	1080
Grieta	48	244	1822	497	grieta_115.jpg	1920	1080
Grieta	48	44	826	516	grieta_116.jpg	1920	1080
Grieta	321	18	983	725	grieta_117.jpg	1920	1080
Hueco	642	68	1052	935	grieta_118.jpg	1920	1080
Grieta	28	225	1858	482	grieta_119.jpg	1920	1080
Hueco	471	476	982	556	grieta_12.jpg	1920	1080
Hueco	611	155	626	274	grieta_12.jpg	1920	1080
Grieta	33	135	1858	888	grieta_120.jpg	1920	1080
Grieta	44	238	1826	446	grieta_121.jpg	1920	1080
Hueco	658	361	123	117	grieta_122.jpg	1920	1080
Hueco	726	350	482	329	grieta_123.jpg	1920	1080
Hueco	729	258	248	90	grieta_124.jpg	1920	1080
Grieta	122	348	1725	326	grieta_125.jpg	1920	1080
Grieta	201	356	376	262	grieta_126.jpg	1920	1080
Grieta	1016	476	639	287	grieta_126.jpg	1920	1080
Hueco	514	462	852	499	grieta_127.jpg	1920	1080
Grieta	1399	411	461	391	grieta_127.jpg	1920	1080
Grieta	386	378	1325	636	grieta_128.jpg	1920	1080
Hueco	104	57	1089	993	grieta_129.jpg	1920	1080
Hueco	221	437	765	323	grieta_13.jpg	1920	1080
Hueco	497	24	256	73	grieta_13.jpg	1920	1080
Hueco	128	129	374	167	grieta_13.jpg	1920	1080
Hueco	577	149	478	170	grieta_13.jpg	1920	1080
Hueco	1451	224	439	321	grieta_13.jpg	1920	1080
Hueco	207	810	997	259	grieta_13.jpg	1920	1080
Hueco	1466	74	321	94	grieta_13.jpg	1920	1080
Grieta	137	15	1212	856	grieta_130.jpg	1920	1080
Grieta	36	18	731	362	grieta_131.jpg	1920	1080
Grieta	923	336	876	334	grieta_131.jpg	1920	1080
Grieta	1579	529	304	150	grieta_132.jpg	1920	1080
Grieta	287	93	1395	637	grieta_133.jpg	1920	1080
Grieta	36	32	809	996	grieta_134.jpg	1920	1080
Grieta	884	15	946	1010	grieta_134.jpg	1920	1080
Hueco	429	34	768	594	grieta_135.jpg	1920	1080
Grieta	179	409	1663	281	grieta_136.jpg	1920	1080
Grieta	87	397	810	187	grieta_137.jpg	1920	1080
Grieta	997	492	904	196	grieta_137.jpg	1920	1080
Grieta	64	386	1805	285	grieta_138.jpg	1920	1080
Hueco	276	32	1563	765	grieta_139.jpg	1920	1080
Grieta	37	875	683	157	grieta_139.jpg	1920	1080
Hueco	106	49	938	405	grieta_14.jpg	1920	1080
Hueco	136	524	745	482	grieta_14.jpg	1920	1080
Hueco	940	517	790	547	grieta_14.jpg	1920	1080
Hueco	170	197	1398	743	grieta_140.jpg	1920	1080
Hueco	561	208	439	458	grieta_141.jpg	1920	1080
Grieta	1100	521	778	464	grieta_141.jpg	1920	1080
Hueco	670	355	549	343	grieta_142.jpg	1920	1080
Hueco	1442	205	266	377	grieta_142.jpg	1920	1080
Grieta	1356	668	358	380	grieta_142.jpg	1920	1080
Grieta	30	417	323	379	grieta_142.jpg	1920	1080
Grieta	86	138	539	218	grieta_142.jpg	1920	1080
Hueco	1183	395	327	214	grieta_143.jpg	1920	1080
Hueco	268	521	240	148	grieta_143.jpg	1920	1080
Grieta	550	395	413	195	grieta_143.jpg	1920	1080
Grieta	1172	672	224	390	grieta_143.jpg	1920	1080
Hueco	62	523	425	461	grieta_144.jpg	1920	1080
Hueco	22	690	307	372	grieta_145.jpg	1920	1080
Hueco	128	213	1043	708	grieta_146.jpg	1920	1080
Hueco	299	440	1527	549	grieta_147.jpg	1920	1080
Hueco	195	149	1641	899	grieta_148.jpg	1920	1080
Grieta	42	309	1337	315	grieta_149.jpg	1920	1080
Grieta	1488	245	405	290	grieta_149.jpg	1920	1080
Hueco	492	116	293	157	grieta_15.jpg	1920	1080
Hueco	918	34	224	92	grieta_15.jpg	1920	1080
Grieta	1661	309	104	598	grieta_15.jpg	1920	1080
Grieta	305	325	1276	441	grieta_150.jpg	1920	1080
Grieta	47	334	1811	330	grieta_151.jpg	1920	1080
Grieta	48	272	1636	636	grieta_152.jpg	1920	1080
Hueco	745	314	1002	455	grieta_153.jpg	1920	1080
Grieta	1613	13	137	220	grieta_153.jpg	1920	1080
Hueco	20	423	365	305	grieta_153.jpg	1920	1080
Hueco	302	286	1032	464	grieta_154.jpg	1920	1080

Clase	Matriz				Nombre de imagen y tipo de extension	Ancho	Altura
Grieta	95	127	1764	757	grieta_155.jpg	1920	1080
Grieta	67	88	1789	767	grieta_156.jpg	1920	1080
Grieta	505	325	1398	438	grieta_157.jpg	1920	1080
Grieta	51	278	1823	402	grieta_158.jpg	1920	1080
Grieta	65	274	1686	450	grieta_159.jpg	1920	1080
Hueco	126	104	1027	751	grieta_16.jpg	1920	1080
Grieta	55	350	1599	377	grieta_160.jpg	1920	1080
Hueco	899	384	189	435	grieta_161.jpg	1920	1080
Hueco	807	79	129	154	grieta_161.jpg	1920	1080
Grieta	33	311	1830	383	grieta_162.jpg	1920	1080
Grieta	50	263	1831	365	grieta_163.jpg	1920	1080
Grieta	51	384	1588	315	grieta_164.jpg	1920	1080
Grieta	898	99	210	977	grieta_165.jpg	1920	1080
Grieta	466	15	913	277	grieta_166.jpg	1920	1080
Hueco	991	328	399	268	grieta_166.jpg	1920	1080
Hueco	444	342	181	165	grieta_166.jpg	1920	1080
Hueco	634	884	142	128	grieta_166.jpg	1920	1080
Hueco	62	501	171	104	grieta_166.jpg	1920	1080
Grieta	83	155	1730	874	grieta_167.jpg	1920	1080
Grieta	190	76	1663	949	grieta_168.jpg	1920	1080
Grieta	142	316	1713	265	grieta_169.jpg	1920	1080
Hueco	1217	699	299	179	grieta_17.jpg	1920	1080
Hueco	798	161	1007	207	grieta_17.jpg	1920	1080
Grieta	94	66	1788	639	grieta_170.jpg	1920	1080
Grieta	142	35	1713	1007	grieta_171.jpg	1920	1080
Grieta	366	124	1292	785	grieta_172.jpg	1920	1080
Hueco	664	395	706	492	grieta_173.jpg	1920	1080
Grieta	143	27	1505	1001	grieta_174.jpg	1920	1080
Grieta	123	253	1515	418	grieta_175.jpg	1920	1080
Hueco	50	55	634	793	grieta_176.jpg	1920	1080
Hueco	711	188	203	268	grieta_176.jpg	1920	1080
Hueco	42	21	1540	856	grieta_177.jpg	1920	1080
Hueco	288	7	1373	589	grieta_178.jpg	1920	1080
Hueco	296	175	1256	684	grieta_179.jpg	1920	1080
Hueco	45	32	1308	919	grieta_18.jpg	1920	1080
Hueco	140	23	1675	865	grieta_180.jpg	1920	1080
Hueco	117	35	1727	712	grieta_181.jpg	1920	1080
Grieta	51	19	1744	983	grieta_182.jpg	1920	1080
Grieta	92	30	1738	991	grieta_183.jpg	1920	1080
Hueco	117	76	1548	965	grieta_184.jpg	1920	1080
Grieta	50	27	1649	510	grieta_185.jpg	1920	1080
Hueco	740	562	284	418	grieta_185.jpg	1920	1080
Grieta	100	30	1326	690	grieta_186.jpg	1920	1080
Hueco	123	397	1753	642	grieta_187.jpg	1920	1080
Hueco	126	306	1466	672	grieta_188.jpg	1920	1080
Hueco	365	297	1206	681	grieta_189.jpg	1920	1080
Hueco	246	44	1524	923	grieta_19.jpg	1920	1080
Hueco	50	80	1488	835	grieta_190.jpg	1920	1080
Hueco	175	60	746	784	grieta_191.jpg	1920	1080
Hueco	34	163	1308	826	grieta_192.jpg	1920	1080
Hueco	672	76	669	563	grieta_193.jpg	1920	1080
Hueco	517	182	92	84	grieta_193.jpg	1920	1080
Hueco	78	30	934	665	grieta_194.jpg	1920	1080
Hueco	443	199	935	703	grieta_195.jpg	1920	1080
Hueco	209	258	199	581	grieta_195.jpg	1920	1080
Hueco	1135	520	483	443	grieta_196.jpg	1920	1080
Hueco	1200	54	658	715	grieta_197.jpg	1920	1080
Hueco	508	454	968	502	grieta_198.jpg	1920	1080
Hueco	592	35	799	595	grieta_199.jpg	1920	1080
Hueco	391	651	349	415	grieta_199.jpg	1920	1080
Hueco	67	741	228	293	grieta_199.jpg	1920	1080
Hueco	664	225	503	505	grieta_2.jpg	1920	1080
Grieta	929	465	72	175	grieta_20.jpg	1920	1080
Hueco	374	197	1378	686	grieta_200.jpg	1920	1080
Hueco	164	163	1487	775	grieta_201.jpg	1920	1080
Grieta	112	456	1627	285	grieta_21.jpg	1920	1080
Hueco	1454	499	243	137	grieta_22.jpg	1920	1080
Hueco	215	46	700	318	grieta_23.jpg	1920	1080
Hueco	246	378	1060	566	grieta_23.jpg	1920	1080
Hueco	284	19	1340	1008	grieta_24.jpg	1920	1080
Hueco	171	741	123	173	grieta_24.jpg	1920	1080
Hueco	720	138	580	541	grieta_25.jpg	1920	1080
Hueco	729	125	874	849	grieta_26.jpg	1920	1080
Hueco	28	426	650	538	grieta_26.jpg	1920	1080
Hueco	793	389	511	482	grieta_27.jpg	1920	1080
Hueco	447	150	630	729	grieta_28.jpg	1920	1080
Hueco	262	454	801	218	grieta_29.jpg	1920	1080
Hueco	64	295	1060	358	grieta_3.jpg	1920	1080
Hueco	436	365	1036	394	grieta_30.jpg	1920	1080
Hueco	148	297	288	207	grieta_31.jpg	1920	1080
Hueco	26	529	999	246	grieta_32.jpg	1920	1080
Hueco	1006	341	92	319	grieta_32.jpg	1920	1080
Grieta	545	461	714	112	grieta_33.jpg	1920	1080
Grieta	214	409	1424	195	grieta_34.jpg	1920	1080
Grieta	486	627	898	182	grieta_34.jpg	1920	1080
Hueco	226	30	1247	787	grieta_35.jpg	1920	1080
Grieta	641	616	759	140	grieta_36.jpg	1920	1080
Hueco	951	484	209	156	grieta_37.jpg	1920	1080
Grieta	62	370	1412	365	grieta_38.jpg	1920	1080
Grieta	61	375	516	209	grieta_39.jpg	1920	1080
Hueco	993	302	221	187	grieta_39.jpg	1920	1080
Hueco	1543	77	179	162	grieta_39.jpg	1920	1080
Hueco	279	72	1063	521	grieta_4.jpg	1920	1080
Hueco	266	34	1256	944	grieta_40.jpg	1920	1080
Hueco	623	372	419	146	grieta_41.jpg	1920	1080
Hueco	1523	786	143	143	grieta_41.jpg	1920	1080
Hueco	432	383	137	69	grieta_41.jpg	1920	1080
Hueco	818	394	569	291	grieta_42.jpg	1920	1080
Hueco	1272	730	153	168	grieta_42.jpg	1920	1080
Hueco	1452	694	128	150	grieta_42.jpg	1920	1080

Clase	Matriz				Nombre de imagen y tipo de extension	Ancho	Altura
Grieta	270	27	1473	1008	grieta_43.jpg	1920	1080
Grieta	203	280	1334	349	grieta_44.jpg	1920	1080
Hueco	103	367	196	304	grieta_45.jpg	1920	1080
Hueco	285	387	156	248	grieta_45.jpg	1920	1080
Hueco	533	68	1043	831	grieta_45.jpg	1920	1080
Hueco	1194	418	137	189	grieta_46.jpg	1920	1080
Hueco	644	507	92	111	grieta_46.jpg	1920	1080
Hueco	449	406	95	112	grieta_46.jpg	1920	1080
Grieta	1267	546	522	380	grieta_47.jpg	1920	1080
Grieta	390	803	171	142	grieta_47.jpg	1920	1080
Grieta	58	404	1611	248	grieta_48.jpg	1920	1080
Hueco	676	450	192	162	grieta_49.jpg	1920	1080
Grieta	329	26	1286	930	grieta_5.jpg	1920	1080
Hueco	391	562	170	190	grieta_50.jpg	1920	1080
Hueco	887	192	140	131	grieta_51.jpg	1920	1080
Grieta	95	280	1747	765	grieta_52.jpg	1920	1080
Grieta	444	464	905	249	grieta_53.jpg	1920	1080
Hueco	977	406	310	168	grieta_54.jpg	1920	1080
Hueco	291	397	344	290	grieta_54.jpg	1920	1080
Grieta	73	124	1717	454	grieta_55.jpg	1920	1080
Grieta	78	294	1767	541	grieta_56.jpg	1920	1080
Hueco	56	325	315	260	grieta_57.jpg	1920	1080
Hueco	1052	10	469	561	grieta_57.jpg	1920	1080
Hueco	452	621	181	204	grieta_57.jpg	1920	1080
Hueco	669	662	151	128	grieta_57.jpg	1920	1080
Hueco	330	336	1340	653	grieta_58.jpg	1920	1080
Grieta	33	355	1417	454	grieta_59.jpg	1920	1080
Grieta	111	35	1348	447	grieta_6.jpg	1920	1080
Hueco	419	166	405	368	grieta_60.jpg	1920	1080
Grieta	491	378	782	432	grieta_61.jpg	1920	1080
Grieta	415	442	421	237	grieta_62.jpg	1920	1080
Grieta	454	29	940	270	grieta_63.jpg	1920	1080
Hueco	1270	434	432	358	grieta_63.jpg	1920	1080
Grieta	114	297	1728	348	grieta_64.jpg	1920	1080
Grieta	95	403	1624	265	grieta_65.jpg	1920	1080
Grieta	140	461	1625	220	grieta_66.jpg	1920	1080
Hueco	740	334	404	295	grieta_67.jpg	1920	1080
Grieta	140	499	369	106	grieta_68.jpg	1920	1080
Grieta	1041	423	732	204	grieta_68.jpg	1920	1080
Grieta	86	412	1658	201	grieta_69.jpg	1920	1080
Hueco	550	261	812	728	grieta_7.jpg	1920	1080
Grieta	65	186	1769	224	grieta_70.jpg	1920	1080
Hueco	533	189	720	656	grieta_71.jpg	1920	1080
Grieta	748	10	516	112	grieta_71.jpg	1920	1080
Grieta	309	133	1516	690	grieta_72.jpg	1920	1080
Grieta	41	320	1479	424	grieta_73.jpg	1920	1080
Grieta	1602	250	295	179	grieta_73.jpg	1920	1080
Grieta	185	303	1636	323	grieta_74.jpg	1920	1080
Grieta	171	219	943	319	grieta_75.jpg	1920	1080
Hueco	139	838	114	98	grieta_76.jpg	1920	1080
Hueco	457	517	101	90	grieta_76.jpg	1920	1080
Hueco	919	210	118	98	grieta_76.jpg	1920	1080
Hueco	1231	532	164	123	grieta_76.jpg	1920	1080
Hueco	659	219	122	118	grieta_77.jpg	1920	1080
Hueco	866	337	151	123	grieta_77.jpg	1920	1080
Hueco	1089	266	173	181	grieta_77.jpg	1920	1080
Hueco	1311	390	168	145	grieta_77.jpg	1920	1080
Hueco	1275	135	112	126	grieta_77.jpg	1920	1080
Hueco	877	735	189	132	grieta_77.jpg	1920	1080
Grieta	23	256	1783	502	grieta_78.jpg	1920	1080
Grieta	536	383	899	252	grieta_79.jpg	1920	1080
Hueco	405	90	1228	891	grieta_8.jpg	1920	1080
Grieta	198	274	413	120	grieta_80.jpg	1920	1080
Grieta	42	66	1822	854	grieta_81.jpg	1920	1080
Hueco	1008	235	329	284	grieta_82.jpg	1920	1080
Grieta	450	322	516	223	grieta_82.jpg	1920	1080
Grieta	1384	351	489	209	grieta_82.jpg	1920	1080
Hueco	28	389	429	477	grieta_82.jpg	1920	1080
Hueco	651	345	475	305	grieta_83.jpg	1920	1080
Hueco	807	557	223	176	grieta_84.jpg	1920	1080
Hueco	1423	323	217	134	grieta_84.jpg	1920	1080
Hueco	1435	211	168	140	grieta_85.jpg	1920	1080
Grieta	1027	365	232	115	grieta_85.jpg	1920	1080
Grieta	1565	15	238	296	grieta_86.jpg	1920	1080
Grieta	1638	501	146	510	grieta_86.jpg	1920	1080
Grieta	196	429	410	153	grieta_86.jpg	1920	1080
Grieta	396	219	329	81	grieta_86.jpg	1920	1080
Grieta	1124	225	204	198	grieta_86.jpg	1920	1080
Grieta	391	623	277	366	grieta_87.jpg	1920	1080
Grieta	648	206	332	78	grieta_87.jpg	1920	1080
Grieta	647	400	380	173	grieta_87.jpg	1920	1080
Grieta	209	325	907	439	grieta_88.jpg	1920	1080
Grieta	1175	99	676	206	grieta_88.jpg	1920	1080
Hueco	1130	772	136	173	grieta_88.jpg	1920	1080
Grieta	436	185	1309	228	grieta_89.jpg	1920	1080
Hueco	229	119	1097	514	grieta_9.jpg	1920	1080
Grieta	154	225	1666	296	grieta_90.jpg	1920	1080
Hueco	424	233	482	455	grieta_91.jpg	1920	1080
Grieta	583	177	1256	524	grieta_92.jpg	1920	1080
Grieta	299	754	256	312	grieta_92.jpg	1920	1080
Hueco	363	238	798	631	grieta_93.jpg	1920	1080
Grieta	586	376	1036	215	grieta_94.jpg	1920	1080
Grieta	143	164	1523	500	grieta_95.jpg	1920	1080
Grieta	477	688	424	376	grieta_95.jpg	1920	1080
Grieta	1166	319	647	209	grieta_96.jpg	1920	1080
Grieta	496	302	1312	402	grieta_97.jpg	1920	1080
Grieta	899	277	963	243	grieta_98.jpg	1920	1080
Grieta	256	439	454	115	grieta_98.jpg	1920	1080
Grieta	265	200	1510	594	grieta_99.jpg	1920	1080

Fig. 5: Image to Matrix Conversion

3.3. Network Architecture Model

Before the improvement and optimization of the model, the YOLO v5x model was selected due to the high degree of precision in the mean, compared to other versions of the same algorithm, being the most appropriate for processing large batches and complex matrix calculations, the algorithm proposed by Le et al. (2022) was taken, which is a variant of the algorithm.

Thus, an improvement in the development of the semantic segmentation architecture and the modules of the CNNs was proposed, using best practices (Ramalingam et al. 2021; Sun et al. 2021) for the data collection process, which served to train the algorithm. The training consisted of 120 epochs and using the Adam optimization algorithm, with images of 1920 x1080. In addition, masks of recurrent convolutional neural networks were added to optimize the process, that is, the obtainments of the characteristics of the lower layer were acquired through the semantic segmentation that adopts the characteristics of the cracks or gaps, as can be seen in figure 6.

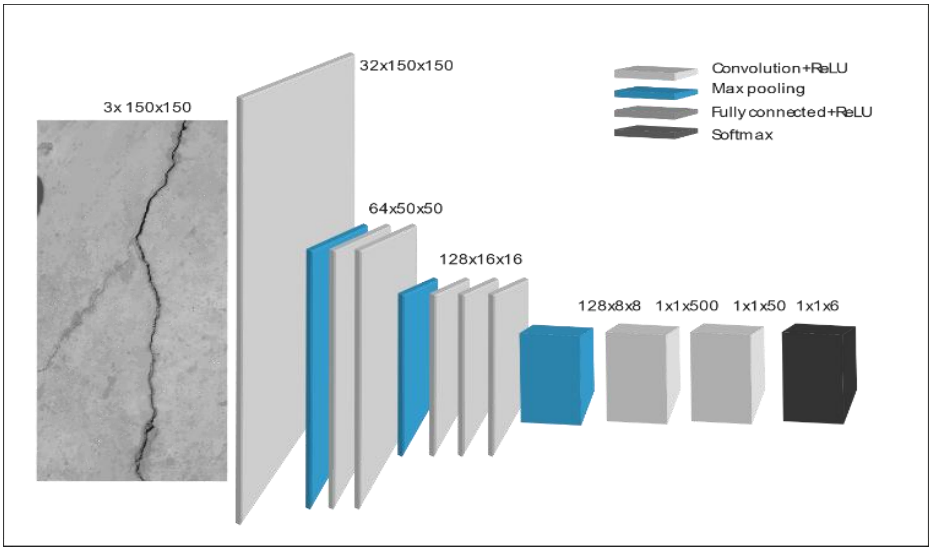

Fig. 6: Adaptación del modelo estructurado de red neuronal convolucional multicapas (Ramalingam et al. 2021; Sun et al. 2021)

Figure 6 presents an adaptation of the YOLO model used for this article, in the first stage the image of the crack or hole was entered, then convolutional operations were performed with the ReLu activation function to eliminate the negatives and proceed to apply the max pooling algorithm for the grouping of the values and achieve an optimal analysis, Finally, segmentation was done through multiple custom layers and the Softmax binary function, which allowed a reduction in the process to mitigate complexity.

3.4. Algorithm Training and Verification

To start with the training process, CNN models were applied for regression and classification, for which 80% of 420 images were used for training, stored in the dataset called dataset_clasificadorGH and in a file the coordinates, to then be entered into the YOLO v5 algorithm, measuring the results using evaluation metrics such as precision (1), of recall (2), accuracy and F1-Score (3), calculating the function of the true positives called in its abbreviation (TP), true negatives (TN), false positives (FP) and false negatives (FN), as follows structurally.

$$Precision = \frac{TP}{TP + FP} \tag{1}$$

$$Recall = \frac{TP}{TP + FN} \tag{2}$$

$$F1 = \frac{2xPrecision\ x\ Recall}{Precision + Recall} \tag{3}$$

Training results obtained from precision (Opara et al., 2021; Kumar et al., 2021; Mukhopadhyay et al., 2021; He & Liu, 2020), are seen in Figure 7.

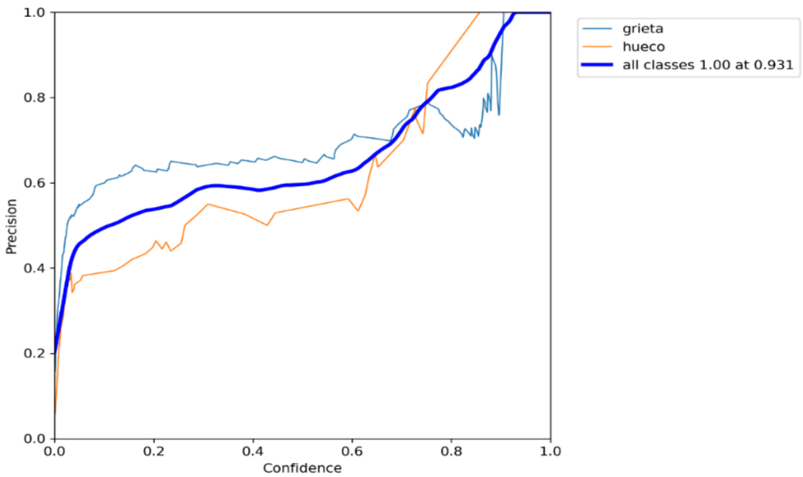

Fig. 7: Precision and Confidence

As shown in Figure 7, the mean accuracy of the crack and hollow classes reached higher values of 0.75, which indicates an optimal behavior of the results for the crack or hollow classes, which can be mentioned that the greater the reliability the accuracy is also higher.

The training results obtained for the Recall (Opara et al., 2021; Kumar et al., 2021; Mukhopadhyay et al., 2021; He & Liu, 2020), are seen in Figure 8.

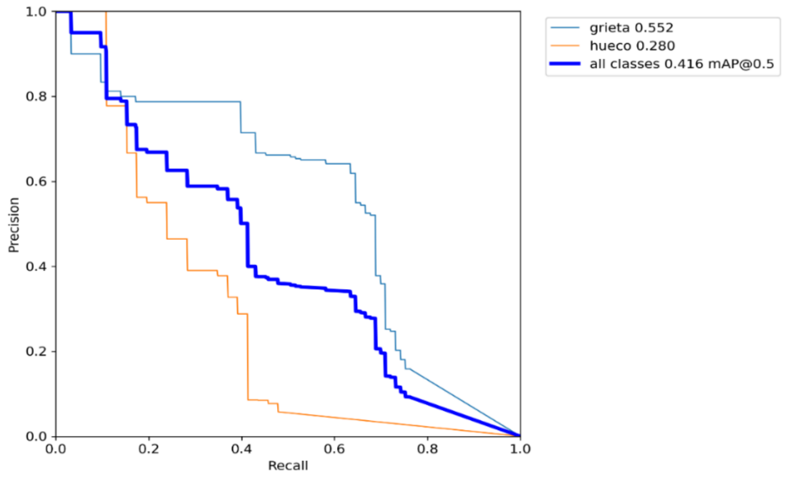

Fig. 8: Recall and Precision

In figure 8, the results obtained from the recall are observed, for cracks and gaps of 0.552 and 0.280 respectively.

The training results obtained for the F1 - score (Opara et al., 2021; Kumar et al., 2021; Mukhopadhyay et al., 2021; He & Liu, 2020), are seen in Figure 9.

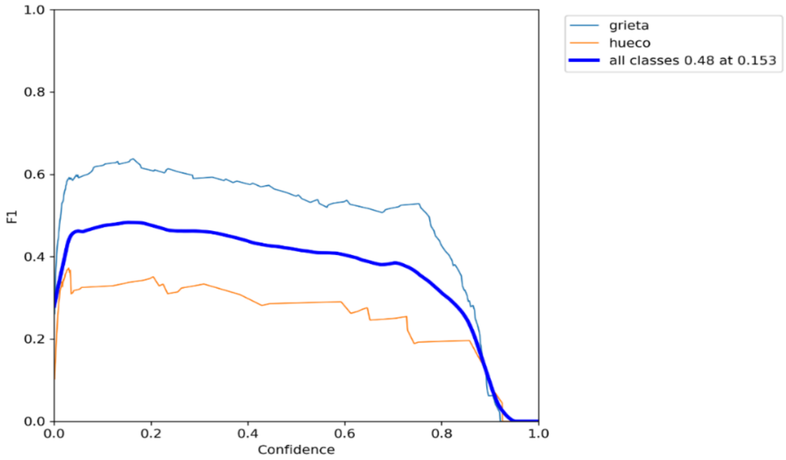

Fig. 9: Score Curve (F1)

In figure 9, the F1-Score of the crack and gap classes is shown, obtaining the results of the precision and the recall, where the F1-score metric for crack has a higher average of 0.5 and the hollow class a higher average of 0.3, which can be said that the higher the reliability, the lower the F1-score.

The results of the training obtained are represented in the confusion matrix, shown in Figure 10.

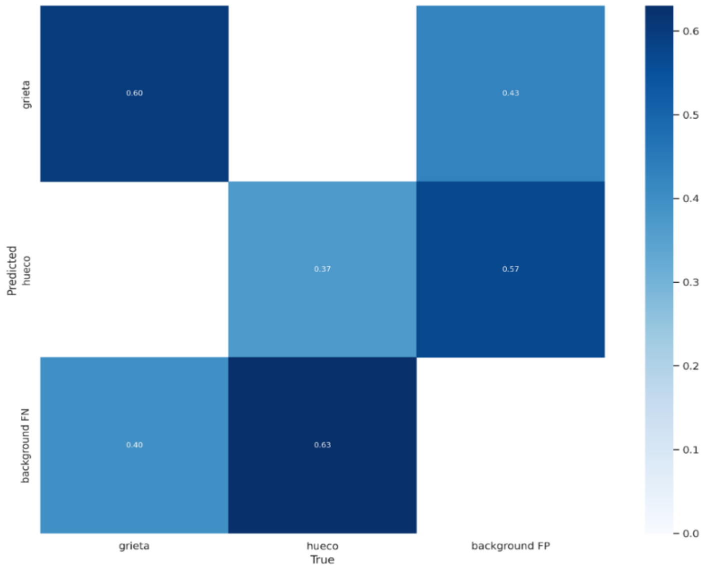

Fig. 10: Confusion matrix

Figure 10, shows the confusion matrix, where it is observed with respect to the crack class for training, obtaining a 0.6 of success and a 0.4 of erroneous prediction, likewise, with respect to the hollow class, a 0.37 of success was obtained in the prediction and a 0.63 of the images that could not be predicted correctly, But they belonged to the hollow class. Thus, the images that do not belong to any class, the 0.57 of the images had an erroneous prediction as hollow class and 0.43 as a crack class.

Then we proceeded to the validation of the model using 20% of the 420 images and 120 epochs, managing to obtain the accuracy and recall metrics, shown in figure 11.

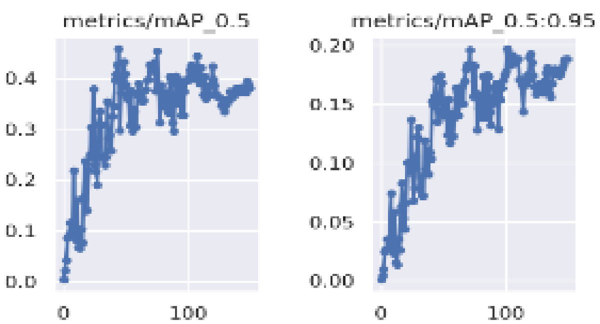

Precision Recall

Fig. 11: Result of Validation

Figure 11 shows the validation of the model, which obtained an average accuracy greater than 0.37 and the recall greater than 0.17.

In Figure 12, the accuracy of some images is visualized, where the hollow class (1) was 36.67%, while for the crack class (0) 63.33%.

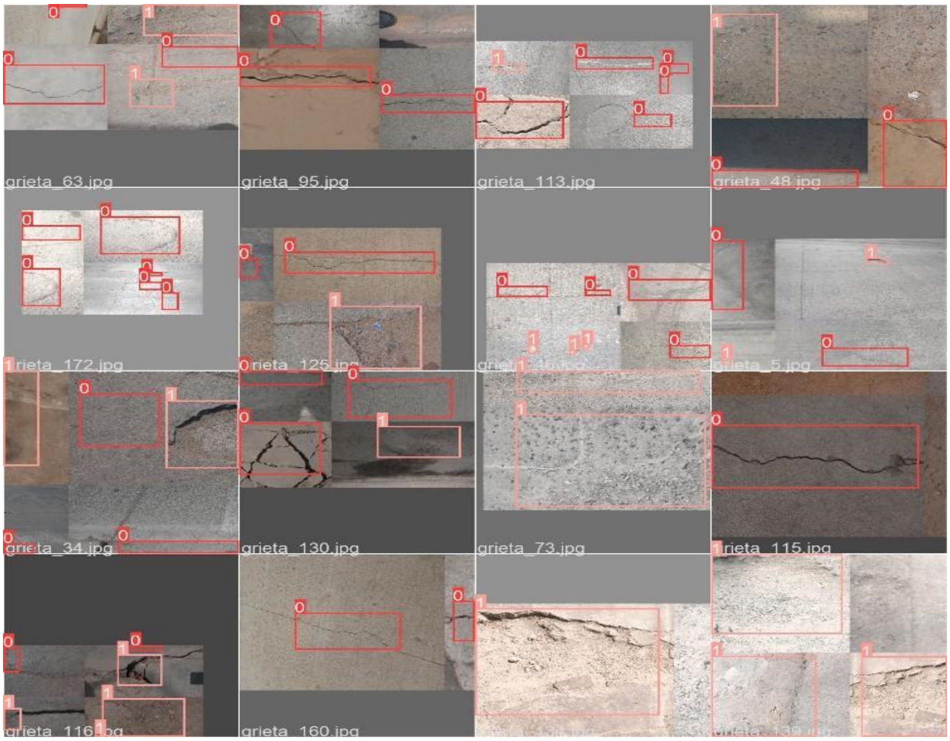

Fig. 12: Validation by Class

3.5. Despliegue

For the test of the model, a system was developed using free libraries such as PyTorch, Python, Cv2, pandas and yaml, which were executed in Google Colab, and for testing on a CPU (Central Processing Unit) Intel(R) Core (TM) i7-10700 (2.90GHz) RAM 16GB with Windows 10 operating system (based on 64 bits).

To develop the system interface, technological tools such as PyCharm Community Edition in its version 2022.1.2, Spyder in its version 4, Anaconda were used. Classified the technological tools, we proceeded with the writing of the code under the Python programming language and the incorporation of the trained model.

Thus, the system started with the user and password entry as shown in Figure 13.

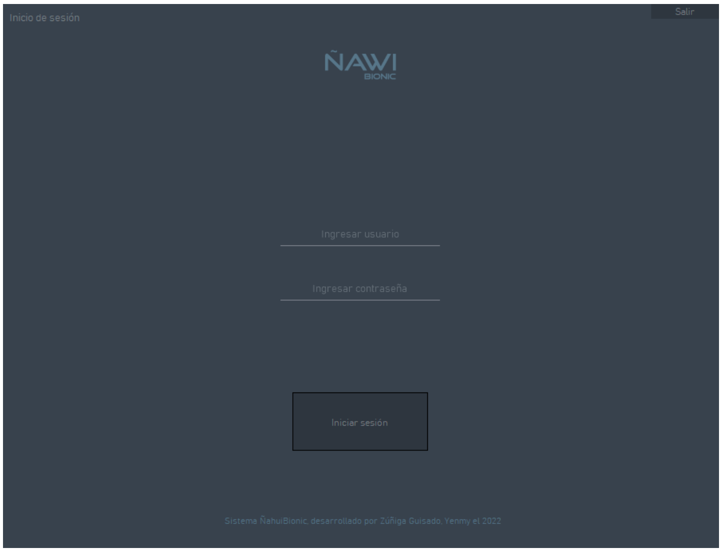

Fig. 13: User Login Interface

En la figura 13, se visualiza una ventana donde permitió validar el registro del usuario y contraseña para el inicio de sesión, desarrollada bajo el lenguaje Python.

Once the system allows access, the interface is shown as in Figure 14, which served to process the images and send them to the trained model.

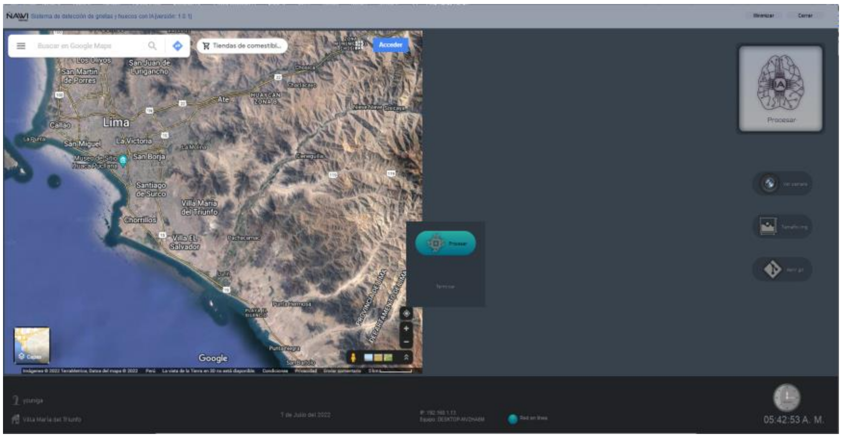

Fig. 14: Main screen to start the model.

In figure 14, the main module is presented, which allowed to capture the image of the pavement, for this the Google Maps API was used that helped to geographically locate the study areas to capture the image of the pavement, as shown in figure 15, whose captured image was sent to the algorithm trained to detect cracks and gaps, for which file routing through Git software was implemented.

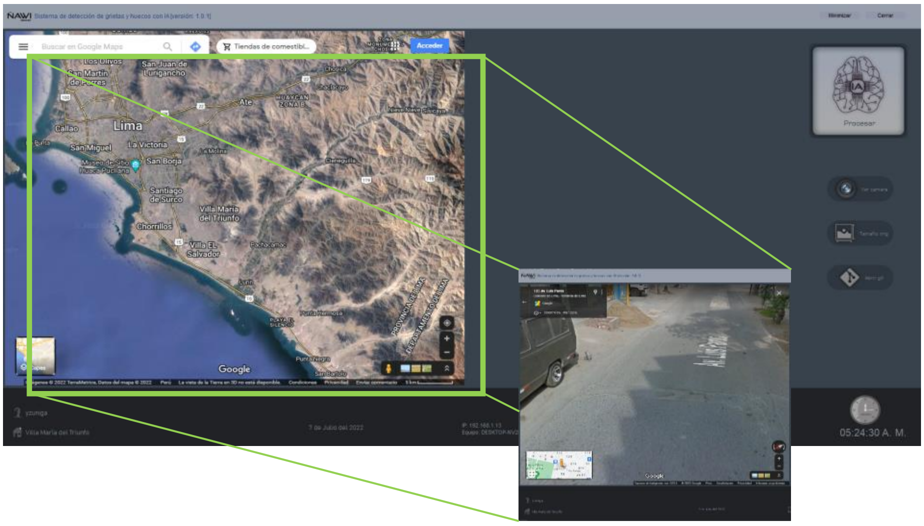

Fig. 15: Image Capture of the Pavement

In figure 15, the operation of the system is visualized to locate a specific area and be able to take an image of the pavement, where later the image was sent to the algorithm for the detection of gaps and cracks in the pavement.

4. Test Results

For the algorithm test, 30 images were used in order to evaluate performance through the metrics: Precision, sensitivity and F1 – score, visualized in Table 3.

Table 3: Resumen de indicadores Test.

Metrics	Failure Type	Result
Precision	Crack	0.93
	Hollow	0.77
Sensitivity	Crack	0.92
	Hollow	0.91
F1-Score	Crack	0.86
	Hollow	0.77

Table 3 shows the result of the metrics, for the crack class there was 0.93 precision, 0.92 sensitivity and 0.86 F1-Score, also in the hollow class it was 0.77 precision, 0.91 sensitivity and 0.77 F1 – score.

Also, the results of the ROC curve by class were analyzed in Figure 16 and 17.

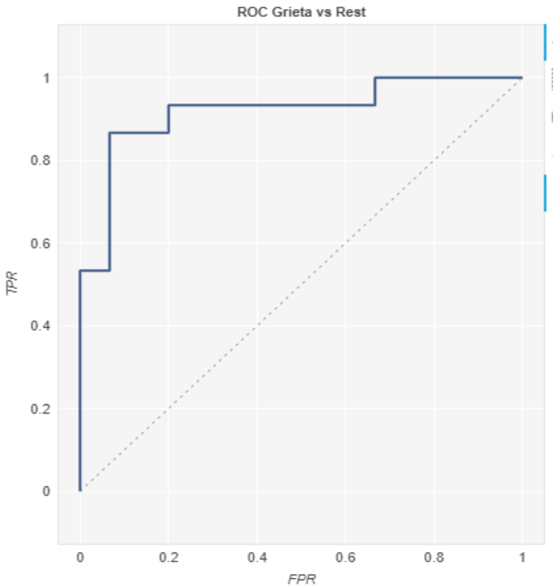

Fig. 16: ROC Crack Curve

In Figure 16, the ROC curve of the crack class is displayed, with an area under the curve greater than 0.5, which allows an optimal result to be deduced.

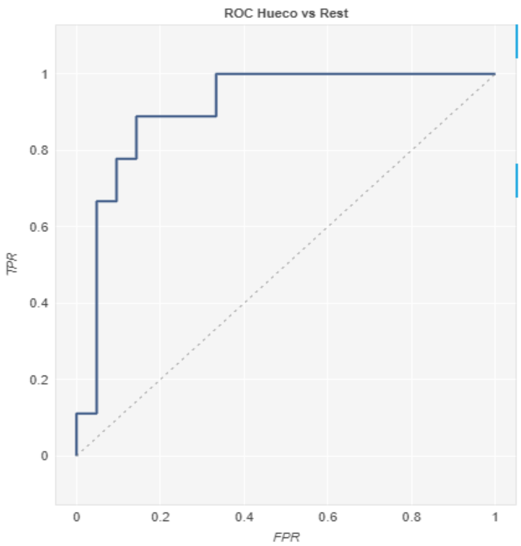

Fig. 17: Hollow ROC Curve

In Figure 17, the ROC curve of the hollow class is displayed, with an area under the curve greater than 0.5, which allows an optimal result to be deduced.

As a last result, the confusion matrix that allowed the analysis of the confusion by classes that the model had, as can be seen in Figure 18.

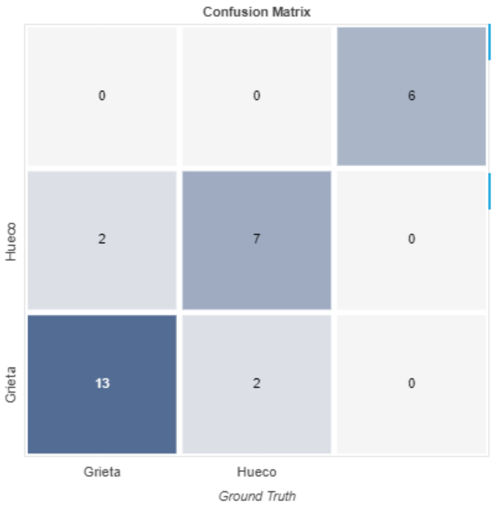

Fig. 18: Confusion Matrix

Figure 18 shows the confusion matrix, where it can be seen that, out of a total of 15 cracks, 13 and 2 incorrect cracks have been correctly detected; In relation to the gaps of a total of 9, 7 were detected correctly and 2 incorrectly; Likewise, it can be seen that 6 characteristics were detected that do not correspond to hollow or crack.

5. Discussion

The results obtained are optimal in the detection of cracks and gaps in the pavement of road structures such as asphalt or concrete for the study area (mainly damaged areas), so a series of processes are carried out applying deep learning techniques and technical tools. As can be seen, some methods tend to study crack detection by capturing static images. Thus, in the results obtained by Fan et al. (2020), the precision reached between 0.19 and 0.92, for the Recall from 0.67 to 0.93, and in F1 it reaches 0.28 to 0.92 in images with resolutions of 768x512, 991x462 and 311x462 pixels. While the metrics obtained in the work were found within the reliability range of metrics between 0.32 and 0.85 in images with a resolution of 1920x1080 pixels.

In the work presented by Fan et al. (2020), a dataset preparation technique was used, involving the cleaning of images that had characteristics of cracks and gaps, as well as other types of failures that can occur on the surface of the road structures to which the technique is applied. Through consolation operations based on the processing of pixel information in an image, crucial for deep learning, it worked similarly to the techniques used to detect cracks and holes in road structures (Opara et al. 2020), being the techniques applied in the development of this work.

The detection of cracks and holes was determined by deep learning and the use of smartphones for image taking, which follows the applied line of this research and that of Maeda et al., (2018), obtaining the objectives raised favorably.

6. Conclusions

From the works applied with artificial intelligence methodologies through deep learning, the present study had positive results, applied through the dataset_clasificadorGH model in the intelligent application, allowing the detection of cracks and gaps, which appear on road traffic surfaces, such as asphalt or concrete structure pavements in different textures or states. Likewise, the model is an alternative solution to the problems that society is going through, detecting dangerous areas for traffic and that can subsequently generate statistical reports, for an adequate analysis by the competent authorities and based on that execute an investment for the rehabilitation of these structures.

It is suggested to use different intelligent models that can be developed with technologies of convolutional neural network structures and sophisticated algorithms such as YOLOv5x. In addition, in the present study indicators were obtained that exceed 50% in the accuracy of detection of cracks and gaps reaching indicators of 86%. On the other hand, during the training, indicators of up to 93% accuracy were obtained, which guarantees the reliability of the model for its implementation in the detection of cracks and gaps, since the studies evaluated and implemented in other countries include records with indicators similar to those obtained.

As limitations of the study were the lack of a suitable device to collect the images, since only a smartphone was available; In addition to the materials that allowed better lighting when capturing the images with the smartphone.

References

Abeliuk, A. & Gutiérrez, C. (2021). Historia y evolución de la inteligencia artificial. 21, 14–21. Retrieved from https://scholar.google.com/scholar?hl=es&as_sdt=0%2C5&q=Historia+y+evoluci%C3%B3n+de+la+inteligencia+artificial&btnG=

Arbaoui, A., Ouahabi, A., Jacques, S., & Hamiane, M. (2021). Concrete Cracks Detection and Monitoring Using Deep Learning-Based Multiresolution Analysis. Electronics, 10(15), 1772. https://doi.org/10.3390/ELECTRONICS10151772

Augustauskas, R. & Lipnickas, A. (2020). Improved Pixel-Level Pavement-Defect Segmentation using a Deep Autoencoder. Sensors 2020, 20(9), 2557. https://www.mdpi.com/1424-8220/20/9/2557/htm

Backman, K., Kulic, D., & Chung, H. (2021). Learning to Assist Drone Landings. IEEE Robotics and Automation Letters, 6(2), 3192–3199. https://doi.org/10.1109/LRA.2021.3062572

Cass, S. (2021). Top Programming Languages: Our Eighth Annual Probe into What's Hot and Not. IEEE Spectrum, 58(10), 17. https://doi.org/10.1109/MSPEC.2021.9563957

Chun, C., & Ryu, S.-K. (2019). Road Surface Damage Detection Using Fully Convolutional Neural Networks and Semi-Supervised Learning. Sensors 2019, Vol. 19, Page 5501, 19(24), 5501. https://doi.org/10.3390/S19245501

Coluccia, A., Fascista, A., Schumann, A., Sommer, L., Dimou, A., Zarpalas, D., & Rajashekar, S. (2021). Drone vs. Bird Detection: Deep Learning Algorithms and Results from a Grand Challenge. Sensors 2021, 1(8), 2824. https://doi.org/10.3390/S21082824

Enzo, R. A., Cassandra, C. R., Felipe, A. N., & Pablo, M. Q. (Eds.). (2021). Artificial Intelligence: Development of Classification and Segmentation Algorithms in Chest Radiography, 27. https://doi.org/10.4067/S0717-93082021000100008

Eslami, E., & Yun, H. B. (2021). Attention-Based Multi-Scale Convolutional Neural Network (A+MCNN) for Multi-Class Classification in Road Images. Sensors 2021, 21(15), 5137. https://doi.org/10.3390/S21155137

Fan, Zhun Lin, Huibiao Li, Chong Su, Jian Bruno, Salvatore Loprencipe, Giuseppe. (2022). Use of Parallel ResNet for High-Performance Pavement Crack Detection and Measurement. Sustainability 2022, 14(3), 1825. https://www.mdpi.com/2071-1050/14/3/1825

Ghaleb, M. S., Ebied, H. M., Shedeed, H. A., & Tolba, M. F. (2022). Image Retrieval Based on Deep Learning. Journal of System and Management Sciences, 12(2), 483–502. https://doi.org/10.33168/JSMS.2022.0226

He, Z., & Liu, Q. (2020). Deep Regression Neural Network for Industrial Surface Defect Detection. IEEE Access, 8, 35583–35591. https://doi.org/10.1109/ACCESS.2020.2975030

Instituto Nacional de Estadística e Infrmática. (2022). Indicador de la Actividad Productiva Departamental - Cuarto Trimestre 2021. Retrieved from https://m.inei.gob.pe/biblioteca-virtual/boletines/produccion-nacional-departamenal-9836/1/#lista

Janani, L., Doley, R., Sunitha, V., & Mathew, S. (2022). Precision Enhancement of Smartphone Sensor-Based Pavement Roughness Estimation By Standardizing host vehicle speed. Canadian Journal of Civil Engineering, 49(6), 716–730. https://doi.org/10.1139/CJCE-2021-0182

Jansen, P. (2022). TIOBE - The Software Quality Company. Retrieved October 9, 2021, from tiobe.com website: https://www.tiobe.com/tiobe-index/

Kim, Y., Song, H., & Han, J. (2022). A Deepfake-Based Deep Learning Algorithm for Medical Data Manipulation Detection. Journal of System and Management Sciences, 12(1), 13–26. https://doi.org/10.33168/JSMS.2022.0102

Kittipongdaja, P., & Siriborvornratanakul, T. (2022). Automatic Kidney Segmentation using 2.5D ResUNet and 2.5D DenseUNet for Malignant Potential Analysis in Complex Renal Cyst based on CT Images. EURASIP Journal on Image and Video Processing, 15. https://doi.org/10.1186/s13640-022-00581-x

Kumar, P., Batchu, S., Swamy S., N., & Kota, S. R. (2021). Real-time Concrete Damage Detection using Deep Learning for High Rise Structures. IEEE Access, 9, 112312–112331. https://doi.org/10.1109/ACCESS.2021.3102647

Ren, L., Lee, Y., Yuen Chai, T., Chua1, S., Lai1, Y., Yee, S., & Haw, S. (2022). Cashierless Checkout Vision System for Smart Retail using Deep Learning. Journal of System and Management Sciences, 12(4), 232-250. https://doi.org/10.33168/JSMS.2022.0415

López, M. T., Fernández-Caballero, A., Mira, J., Delgado, A. E., & Fernández, M. A. (2006). Algorithmic Lateral Inhibition Method in Dynamic and Selective Visual Attention Task: Application to moving objects detection and labelling. Expert Systems with Applications, 31(3), 570–594. https://doi.org/10.1016/j.eswa.2005.09.062

Madasamy, K., Shanmuganathan, V., Kandasamy, V., Lee, M. Y., & Thangadurai, M. (2021). OSDDY: Embedded System-Based Object Surveillance Detection System with Small Drone using Deep YOLO. EURASIP Journal on Image and Video Processing 2021 2021:1, 2021(1), 1–14. https://doi.org/10.1186/S13640-021-00559-1

Maeda, H., Sekimoto, Y., Seto, T., Kashiyama, T., & Omata, H. (2018). Road Damage Detection Using Deep Neural Networks with Images Captured Through a Smartphone. University of Tokyo, 14. https://doi.org/10.48550/arXiv.1801.09454

Morales, T., Sarabakha, A., & Kayacan, E. (Eds.). (2020). Image Generation for Efficient Neural Network Training in Autonomous Drone Racing. https://doi.org/10.1109/IJCNN48605.2020.9206943

Mukhopadhyay, S., Cennamo, N., Deen, M. J., Lee, J., Fabio, T. S., Chen, C., Seo, H. (2021). Deep Learning-Based Thermal Image Analysis for Pavement Defect Detection and Classification Considering Complex Pavement Conditions. Remote Sensing 2022, Vol. 14, Page 106, 14(1), 106. https://doi.org/10.3390/RS14010106

Oliphant, T. (2022). Numpy. Retrieved March 20, 2022, from numpy.org website: https://numpy.org/doc/stable/index.html#

Opara, J. N., Thein, A. B. B., Izumi, S., Yasuhara, H., & Chun, P.-J. (2021). Defect Detection on Asphalt Pavement by Deep Learning. International Journal of GEOMATE, 21(83), 87–94. https://doi.org/10.21660/2021.83.6153

Palma, J. T., & Morales, R. M. (2008). Inteligencia Artificial. Técnicas, métodos y aplicaciones. McGRAW-HILL/INTERAMERICANA DE ESPAÑA, S. A. U.

Park, J., Yoon, D., & Lee, W.-H. (2018). Architectural Factors Detection from Plan by Deep Learning Framework. International Journal of Grid and Distributed Computing, NADIA, 11(1), 57-64, doi: 10.14257/ijgdc.2018.11.1.06.

Qiao, W., Liu, Q., Wu, X., Ma, B., & Li, G. (2021). Automatic Pixel-Level Pavement Crack Recognition Using a Deep Feature Aggregation Segmentation Network with a scSE Attention Mechanism Module. Sensors 2021, 21(9), 2902. https://doi.org/10.3390/S21092902

Qt Group. (2022). Qt. Retrieved from Qt The Qt Company website: https://investors.qt.io/?hsLang=en

Ramalingam, B., Hayat, A. A., Elara, M. R., Gómez, B. F., Yi, L., Pathmakumar, T., Subramanian, S. (2021). Deep Learning Based Pavement Inspection Using Self-Reconfigurable Robot. Sensors 2021, 21(8), 2595. https://doi.org/10.3390/S21082595

Sarmiento-Ramos, J. L. (2020). Aplicaciones de las redes neuronales y el deep learning a la ingeniería biomédica. Revista UIS Ingenierías, 19(4), 1–18. https://doi.org/10.18273/REVUIN.V19N4-2020001

Shatnawi, N. (2018). Automatic Pavement Cracks Detection using Image Processing Techniques and Neural Network. International Journal of Advanced Computer Science and Applications, 9(9), 399–402. https://doi.org/10.14569/IJACSA.2018.090950

Shim, S., Kim, J., Cho, G. C., & Lee, S. W. (2020a). Multiscale and Adversarial Learning-based Semi-Supervised Semantic Segmentation Approach for Crack Detection in Concrete Structures. IEEE Access, 8, 170939–170950. https://doi.org/10.1109/ACCESS.2020.3022786

Silva, L. A., Blas, H. S. S., García, D. P., Mendes, A. S., & González, G. V. (2020). An Architectural Multi-Agent System for a Pavement Monitoring System with Pothole Recognition in UAV Images. Sensors 2020, 20(21), 6205. https://doi.org/10.3390/S20216205

Skalski, P. (2022). Make Alpha Sense. Retrieved June 2, 2022, from Make Alpha Sense.ai website: https://www.makesense.ai/

Srivastava, S., Divekar, A. V., Anilkumar, C., Naik, I., Kulkarni, V., & Pattabiraman, V. (2021). Comparative Analysis of Deep Learning Image Detection Algorithms. Journal of Big Data 2021, 8(1), 1–27. https://doi.org/10.1186/S40537-021-00434-W

Sun, Y., Yang, Y., Yao, G., Wei, F., & Wong, M. (2021). Autonomous Crack and Bughole Detection for Concrete Surface Image based on Deep Learning. IEEE Access, 9, 85709–85720. https://doi.org/10.1109/ACCESS.2021.3088292

Van Rossum, G. (2022). python. Retrieved September 7, 2021, from www.python.org website: https://www.python.org/

Xiao, Y., Daniel, L., & Gashinova, M. (2021). Image Segmentation and Region Classificationin Automotive High-Resolution Radar Imagery. IEEE Sensors Journal, 21(5), 6698–6711. https://doi.org/10.1109/JSEN.2020.3043586

Zhang, L. (2021). Hand-drawn sketch recognition with a double-channel convolutional neural network. EURASIP Journal on Advances in Signal Processing, 2021(1), 1–12. https://doi.org/10.1186/S13634-021-00752-4

Zhang, M., Liu, Y., Luo, S., & Gao, S. (2020). Research on Baidu Street View Road Crack Information Extraction Based on Deep Learning Method. Journal of Physics: Conference Series, 1616(1), 012086. https://doi.org/10.1088/1742-6596/1616/1/012086